EARTH OBSERVATION AND GEOMATICS ENGINEERING
website: https://eoge.ut.ac.ir

Unsupervised building change detection in VHR images using improved PCA-KMeans algorithm

Niloufar Soheili [1], Mahdi Hasanlou [1]*, Masoomeh Gomroki [1]

[1]School of Surveying and Geospatial Engineering, College of Engineering, University of Tehran, Tehran, Iran

Article history:
Received: 2023-03-17, Accepted: 2023-05-01, Published: 2023-06-14

ABSTRACT

While Very High-Resolution (VHR) imagery is favored for change detection due to its spatial detail, it presents challenges, notably intricate feature interactions, and noise, complicating precise change identification. Addressing this, this paper introduces an unsupervised method for detecting building changes in Very High-Resolution (VHR) images, integrating the strengths of Principal Component Analysis (PCA) and K-Means clustering with a focus on building changes. Initially, PCA is employed to reduce data dimensionality, emphasizing the most significant variations across temporal datasets. The difference between the PCA-transformed images is computed, revealing areas of potential change. K-means clustering then categorizes these regions based on their pixel values, labeling them as either changed or unchanged. A unique step in our approach is the building index extraction. This step refines the building detection by identifying contours in the segmented images based on their properties, such as area and perimeter emphasizing true building alterations and filtering out unrelated landscape changes. Experimental results on benchmark datasets, LEVIR-CD and CLCD, showcase the superior performance of the method, with an overall accuracy of 0.97 and a Kappa coefficient of 0.89. These results highlight the effectiveness of the proposed approach for building change detection in remote sensing and urban monitoring applications.

KEYWORDS

Unsupervised Building Change Detection,
VHR images,
PCA-KMeans,
Building Index Mask.

1. Introduction

Earth observation through remote sensing satellites is a crucial tool for understanding human-induced changes on our planet (Saha, Bovolo, & Bruzzone, 2020). Change detection, a dynamic field of research in remote sensing, aims to identify and analyze alterations in the Earth's surface using multitemporal images taken over the same area at different times (Jia, Li, Zhang, Wu, & Zhu, 2016). The timely and accurate detection of land surface changes is essential for comprehending the relationships between human activities and natural phenomena, leading to improved resource management.

Change detection has widespread applications, including natural resource monitoring (H.-C. Li, Celik, Longbotham, & Emery, 2015), agricultural development (Lee, 1981), urban planning and management (Gomroki, Hasanlou, & Reinartz, 2023; S. Wang, You, & Fu, 2011), and disaster

* Corresponding author
E-mail addresses: niloufar.soheili@ut.ac.ir (N. Soheili); hasanlou@ut.ac.ir (M. Hasanlou); masoomeh.gomroki@ut.ac.ir (M Gomroki)

assessment (pang et al.2019; Li et al.2010). In the event of sudden natural disasters, a robust change detection algorithm can swiftly detect subtle changes, enabling immediate action by local governments to minimize human and financial losses. Notably, urban changes are of particular importance due to their impact on resource usage and the well-being of the population.

Very high-resolution satellite imagery has revolutionized change detection applications, providing rich information on colors, textures, and structures of terrestrial objects. Satellites like WorldView, GeoEye, QuickBird, and KOMPSAT, equipped with high-resolution sensors, are widely used for extracting spatial information. Advancements in aerospace and electronic technology continuously improve remote sensing image resolution, meeting the increasing demand for high-resolution optical images in large-scale land cover change analysis. Urban areas are a focal point of research for building change detection. These high-resolution imaging advancements promise a comprehensive understanding of human-induced changes to the Earth's surface.

Change detection methods in remote sensing generally consist of three distinct stages. The first stage is pre-processing, where the main goal is to make images closely aligned and comparable. During this phase, techniques such as co-registration and denoising are applied. (Scheffler, Hollstein, Diedrich, Segl, & Hostert, 2017; Wu et al., 2020). The next step involves forming a difference image (DI) (Saha, Bovolo, & Bruzzone, 2019) using change vector analysis, a technique that calculates pixel differences by examining spectral data. Due to the vast amount of spectral data in multi-spectral images, the process can be computationally demanding. As a solution, Principal Component Analysis (PCA) is often used to select the most relevant features, simplifying the computation (Dharani & Sreenivasulu, 2021; Han, Javed, Jung, & Liu, 2020; Lou, Jia, Yang, & Kasabov, 2019). The final stage is classification, where pixels are labeled as either changed or unchanged. The classification can be done through supervised or unsupervised techniques. Unsupervised methods, which don't require labeled data, are frequently used with common techniques such as thresholding and clustering.

Supervised methods tend to be more accurate because they benefit from learning from a substantial number of labeled samples. However, preparing these labeled samples manually is time-consuming and expensive. Moreover, when natural disasters such as floods, fires, and earthquakes occur, obtaining real and high-quality information is often challenging. As a result, unsupervised methods become more efficient. In this article, the focus is on the utilization of unsupervised methods.

In recent years, many traditional methods have proven successful in change detection. (Celik, 2009) utilized principal component analysis and K-means clustering as a means of change detection. (Celik, 2010) introduced a change-detection method using probabilistic Bayesian inference with the Expectation Maximization (EM) algorithm for parameter estimation to threshold DT-CWT data. In (B. Wang et al., 2015) presented an unsupervised change detection method that utilized cross-sharpening of multitemporal images and image segmentation to reduce errors caused by spatial displacement. (Gu, Lv, & Hao, 2017) proposes an improved Markov random field (MRF), which refines spatial relations and uses linear weights for precise change detection. Another study forms adaptive regions around pixels, subsequently labeling them through the k-means clustering method and refining their identification using an adaptive majority voting technique (Lv, Liu, Shi, Benediktsson, & Du, 2019). Additionally, (Liu, Liu, & Wang, 2017) presents an unsupervised technique for Multi-Spectral image change detection, which combines thresholding with a Gaussian Mixture Model.

Although deep learning has been increasingly applied to change detection, often outperforming traditional methods in accuracy, it still leans on conventional techniques as its foundation. Firstly, bitemporal images are processed using traditional methods like CVA or PCA to derive initial results. These preliminary outcomes then serve as training samples for a deep neural network. In the study, a feature extraction system was introduced, utilizing a feature fusion deep convolutional autoencoder for unsupervised change detection in hyperspectral remote sensing images (HSI) (Seydi et al., 2021). Another strategy proposed by (Q. Li et al., 2021), involves the combination of two complementary model-driven techniques, namely structural similarity (SSIM) that uses K-means and change vector analysis (CVA), to create reliable labels for training a convolutional neural network (CNN).

Principal Component Analysis (PCA) is recognized as a pivotal transformation frequently used in (HSI) change detection (Chen, Wang, Chen, & Deng, 2023; Guo, Zhang, Zhong, & Zhang, 2021; M. Li et al., 2018). In (Z. Wang, Jiang, Liu, Xie, & Li, 2021) utilized an attention-based spatial and spectral network, incorporating PCA-guided self-supervised feature extraction, to achieve improved change detection in (HSI). Moreover, in (Y. Li et al., 2022) (PCA) was used for dimensionality reduction. This reduced data was then processed to derive a different image. For the final step, k-means clustering was applied to the difference image for binary change detection, distinguishing between changed and unchanged regions.

Adapting from hyperspectral image methodologies, this paper applies PCA and k-means clustering to Very High-Resolution (VHR) images, which have inherently fewer bands than (HSI). While these techniques are common for hyperspectral images, their use in VHR is less frequent. Given the complexity of VHR imagery, unsupervised change detection becomes a significant challenge, making this research a valuable contribution to the field of VHR image analysis.

This study aims to advance current unsupervised methods of hyperspectral image change detection specifically for Very High-Resolution (VHR) imagery, addressing its unique challenges. This paper introduces an unsupervised, three-step approach for detecting building changes within VHR images. First, PCA is applied for efficient data dimensionality reduction and the creation of difference image. Next, K-Means clustering is employed to group similar pixels, resulting in a change map. Finally, a building index extraction technique identifies probable building locations. The rest of the paper is organized as follows: In Section 2, the datasets introduced in this study are detailed. Section 3 presents the proposed unsupervised building change detection method. Section 4 showcases the performance evaluation of the approach using various VHR datasets. Finally, Section 5 provides the conclusion to this paper.

2. Datasets

To assess the efficacy of the proposed method, extensive experiments were conducted on two VHR image datasets. The first dataset LEVIR-CD is a large-scale remote sensing building Change Detection dataset, serving as a benchmark for evaluating CD algorithms. It comprises 637 very high-resolution Google Earth image patch pairs (0.5m/pixel), each sized 1024 × 1024 pixels. The bitemporal images span 5 to 14 years, demonstrating notable land-use changes, particularly in terms of building construction. It includes diverse building types and focuses on construction growth and building decline.

The second dataset, known as CLCD, comprises 600 pairs of samples capturing changes in cropland. Collected by the Gaofen-2 satellite over Guangdong Province, China, during 2017 and 2019, the dataset offers images at a spatial resolution ranging from 0.5 to 2 meters. Each sample set contains two images sized 512 × 512 pixels, accompanied by a corresponding binary label denoting the presence or absence of cropland change.

(a) (b) (c)

Figure 1. The LEVIR dataset. (a) Input image $\boldsymbol{X_1}$, (b) Input image $\boldsymbol{X_2}$, and (c) Ground truth image

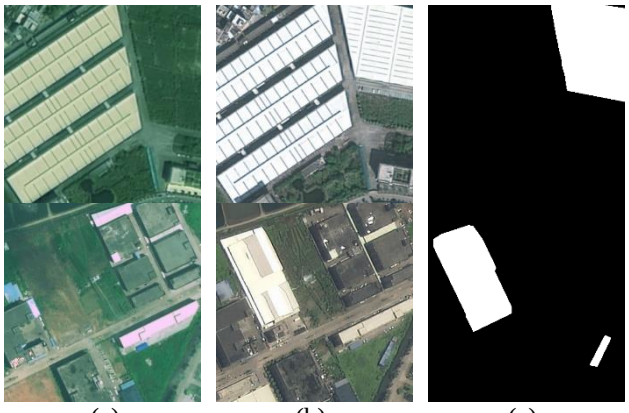

(a) (b) (c)

Figure 2. The CLCD dataset. (a) Input image $\boldsymbol{X_1}$, (b) Input image $\boldsymbol{X_2}$, and (c) Ground truth image

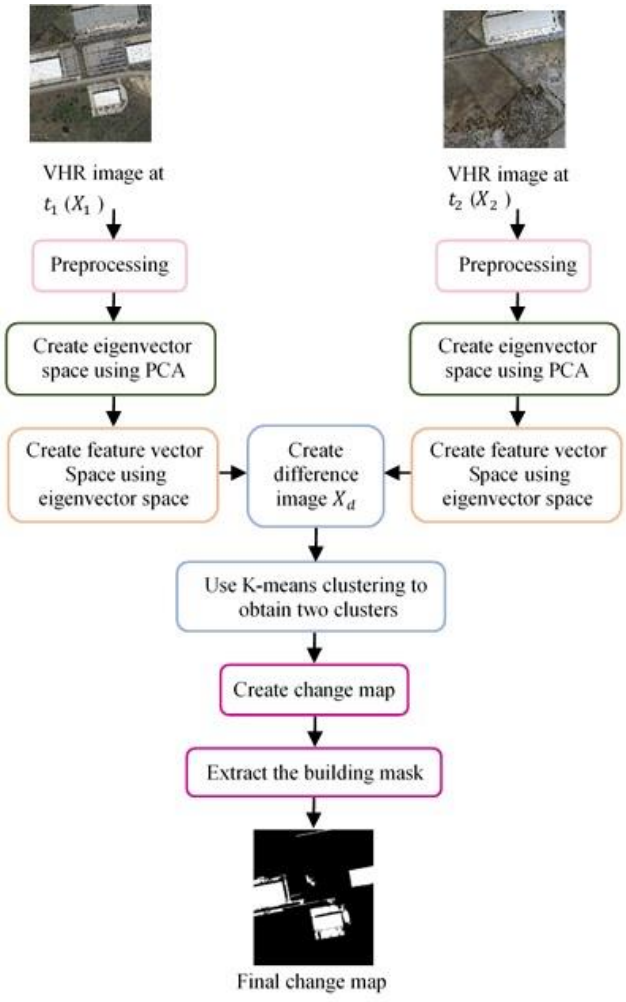

Figure 3. Illustration of the Proposed Unsupervised

3. Methodology

In this study, an unsupervised approach for detecting building changes in Very High-Resolution (VHR) images is presented. The approach begins with Principal Component Analysis (PCA) to reduce image dimensionality, producing a difference image highlighting changes. Feature vectors derived from these transformed images are then clustered using K-Means, resulting in a change map that categorizes regions based on alterations. The resulting labels establish a change map, emphasizing identified changes between the two images.

Additionally, a building index extraction method is utilized. This step takes the change map as its foundation and identifies potential building locations. It works by filtering out noise and retaining contours that match building profiles, ultimately producing a building mask. The combination of these techniques enables efficient change detection and analysis, providing valuable insights for urban planning and environmental monitoring.

The following flowchart provides a visual representation of the key stages of this approach.

3.1. Principal Component Analysis

The method's utilization of Principal Component Analysis (PCA) inherently captures and emphasizes significant terrestrial changes, distinguishing them clearly from minor radiometric or spectral variations. PCA was applied to analyze the flattened vectors of two time-sequential images, image1, and image2, both capturing the same geographical area. The process of deriving these flattened data involved converting the pixel values of the images into one-dimensional vectors. The extraction of principal components effectively reduced dimensionality while preserving critical information. The same PCA model was applied to transform the vectors of image2, ensuring consistency for comparison. Consider two VHR images, denoted as X_1 and X_2, each image acquired at different time instances t_1 and t_2, respectively. The covariance matrix of X_1, as represented in Equation (1), can be expressed as follows:

$$\sum_1 = \frac{1}{n-1} X_1 X_1^T \quad (1)$$

The projection matrix in PCA, as outlined in Equation (2), is primarily computed through the process of eigenvalue decomposition, which allows us to identify the principal components of the data:

$$\sum_1 W_1 = \Lambda_1 W_1 \quad (2)$$

By performing eigenvalue decomposition on $\sum_1$, the eigenvector matrix W_1 and the diagonal matrix of eigenvalues Λ_1 are derived in descending order. Then the corresponding K eigenvectors are collected and arranged as row vectors to create the eigenvector matrix P_1, which effectively represents the principal components. Converting matrix P_1 into the new space spanned by K eigenvectors, resulting in the object matrix in the eigenvector space, reduced to K dimensions, as detailed in Equation (3):

$$Y_1 = P_1 X_1 \quad (3)$$

Likewise, by selecting the top K eigenvalues and their corresponding eigenvectors from $X2$, the reduced-dimensional object matrix in the eigenvector space is constructed, as indicated in Equation (4):

$$Y_2 = P_2 X_2 \quad (4)$$

The difference image, computed from element-wise differences between the reduced vectors of image2 and image1, effectively captured temporal variations. To enhance discrimination and simplify the analysis, the first five principal components were selected as feature vectors. Each pixel in the difference image was represented as a reduced-dimensional feature vector, enabling investigations into spatial patterns and changes. The difference image X_d is obtained by absolute-valued intensity values of these two input images. Subsequently, the K-Means clustering method is employed to segment X_d and obtain the change map, as defined in Equation (5):

$$X_d = |Y_2 - Y_1| \quad (5)$$

3.2. K-Means

In this unsupervised change detection method, K-Means clustering with K = 3 was used to group pixels from the given sample set X_d into two clusters, denoted as C_1 and C_2. Each cluster's centroid μ_i was computed as the mean of the data points within the respective cluster. Cluster C_1 represented the region of change in the difference image X_d, while C_2 represented the region of no change. The Euclidean distance, as calculated by Equation (6), was used by K-Means to iteratively minimize the difference between the eigenvectors and centroids. This approach ensured the effective capturing of essential characteristics.

$$E = \sum_{i=1}^{k} \sum_{x \epsilon c_i} ||X - \mu_i||_2^2 \quad (6)$$

After clustering, centroid-based classification was applied to associate each pixel's feature vector in the difference image with the nearest cluster, resulting in a change map visualizing spatial changes. This approach provided valuable insights into temporal variations without

requiring labeled data, enhancing the understanding of temporal variations within the geographical area.

Following the derivation of the change map from K-Means clustering, the next challenge lies in filtering out changes specific to buildings from other terrestrial alterations. To tackle this, a specialized Building Index Extraction process is introduced. This phase is critical in refining the results of the change detection process. While PCA and K-Means clustering reveal a broad spectrum of alterations in the landscape, they do not discriminate between changes in building structures and other environmental modifications. The Building Index Extraction ensures that these broad changes are further refined to focus specifically on building structures.

3.3. Building Index Extraction

The Building Index Extraction process is designed to extract regions corresponding to buildings from a binary image, leading to the production of a building change detection map. The steps in the process are as follows:

3.3.1. Contour Detection

Contours are defined as continuous points outlining boundaries based on differences in color or intensity. In this study, contours highlight potential building edges in high-resolution images. Recognizing that not all detected contours would correspond to buildings, especially in urban satellite imagery where numerous features might be present, it becomes essential to differentiate genuine building structures. Therefore, the algorithm employs additional refinement steps, using two geometric criteria, to accurately filter out unrelated elements from the image.

3.3.2. Area Threshold

Only contours with an area greater than a predefined minimum are considered. This threshold ensures the exclusion of small noise or irrelevant features that might be falsely identified as buildings.

3.3.3. Perimeter Threshold

The algorithm also considers the perimeter or the length of the contour. Contours with perimeters above a certain threshold are retained. This inclusion criterion aligns contours with the typical dimensions of buildings observable in the imagery.

3.3.4. Building Mask Generation

After filtering, the selected contours are filled to form distinct regions. These regions are subsequently represented on a blank mask, generating what is termed the building mask. This mask provides a clear visual indication of the regions in the binary image, signifying the probable locations of buildings. This building mask is vital for subsequent change detection analysis.

Using contour detection and refinement, the algorithm isolates building structures in binary images, enabling precise change detection pertinent to urban development or transformations.

(a) (b) (c) (d)

Figure 4. The top two rows depict images from the LEVIR dataset, while the bottom two rows showcase images from the CLCD dataset. (a) Input image X_1, (b) Input image X_2 , (c) Change map, and (d) Ground truth image

4. Experimental Results and Analysis

This section conducts an evaluation of the building change detection performance on two distinct datasets: LEVIR and CLCD. Each dataset contains two samples, ensuring comprehensive analysis. The assessment covers both qualitative and quantitative aspects, providing a good understanding of the approach. Using four key metrics, including Overall Accuracy, Kappa, Recall, and F1 Score, the precision of the change detection model in identifying alterations is measured. The summarized outcomes in Table 1 highlight the superior approach, complemented by Fig. 4, which confirms the model's proficiency in visualized change detection results.

These datasets include both isolated and interconnected buildings, presenting various challenges such as shadows, occluded areas, vegetation, and complex roofs. While the performance for isolated buildings is promising, connected buildings pose unique challenges due to shared boundaries and occlusions. As depicted in Fig. 4, The proposed change detection model demonstrates enough robust capabilities to handle the spatial and spectral resolutions of VHR images. It adeptly preserves edges while accurately identifying building shapes and orientations.

The Kappa coefficient is a statistical measure that assesses the agreement between the observed classifications and the expected classifications, In the LEVIR dataset, Kappa values range from 0.65 to 0.67, while in the CLCD dataset, they range from 0.86 to 0.89. Higher Kappa values typically correspond to simpler changes occurring against less complex backgrounds. These values indicate moderate to strong agreement, suggesting reliability in identifying building changes. By referring to Table 1, which provides a summary of these metrics, a better understanding of the significance of these values within the field can be obtained.

Table 1. A summary of the dataset statistics used in this study.

Datasets	Sample	Overall Accuracy	Kappa	Recall	F1 Score
LEVIR	1	0.93	0.67	0.96	0.70
	2	0.92	0.65	0.87	0.69
CLCD	1	0.97	0.89	0.83	0.91
	2	0.97	0.86	0.83	0.87

5. Conclusion

The proposed algorithm stands out for its computational simplicity and remarkable ability to identify significant changes, making it an ideal choice for real-time applications. This research introduces an effective change detection model that accurately identifies changes in the LEVIR and CLCD datasets. The evaluation metrics, including Overall Accuracy, Kappa, Recall, and F1 Score, highlight the model's robust performance. While the algorithm may face challenges in handling complex and dense residential areas, its overall performance makes it a valuable tool for various applications, offering valuable insights for urban planning, environmental monitoring, and disaster management tasks. These discoveries significantly advance the fields of remote sensing and image analysis, opening up new avenues for future research to explore further improvements and advancements.

References

Celik, T. (2009). Multiscale Change Detection in Multitemporal Satellite Images. IEEE Geoscience and Remote Sensing Letters, 6(4), 820–824. https://doi.org/10.1109/LGRS.2009.2026188

Celik, T. (2010). Change Detection in Satellite Images Using a Genetic Algorithm Approach. IEEE Geoscience and Remote Sensing Letters, 7(2), 386–390. https://doi.org/10.1109/LGRS.2009.2037024

Chen, H., Wang, T., Chen, T., & Deng, W. (2023). Hyperspectral Image Classification Based on Fusing S3-PCA, 2D-SSA and Random Patch Network. Remote Sensing, 15(13), 3402. https://doi.org/10.3390/rs15133402

Dharani, M., & Sreenivasulu, G. (2021). Land use and land cover change detection by using principal component analysis and morphological operations in remote sensing applications. International Journal of Computers and Applications, 43(5), 462-471. https://doi.org/10.1080/1206212X.2019.1578068

Gomroki, M., Hasanlou, M., & Reinartz, P. (2023). STCD-EffV2T Unet : Semi Transfer Learning EfficientNetV2 T-Unet Network for Urban/Land Cover Change Detection Using Sentinel-2 Satellite Images. Remote Sensing, 15(5), 1232. https://doi.org/10.3390/rs15051232

Gu, W., Lv, Z., & Hao, M. (2017). Change detection method for remote sensing images based on an improved Markov random field. Multimedia Tools and Applications, 76, 17719-17734.

Guo, Q., Zhang, J., Zhong, C., & Zhang, Y. (2021). Change detection for hyperspectral images via convolutional sparse analysis and temporal spectral unmixing. IEEE Journal of Selected Topics in Applied Earth Observations and Remote Sensing, 14, 4417-4426.

Han, Y., Javed, A., Jung, S., & Liu, S. (2020). Object-Based Change Detection of Very High Resolution Images by Fusing Pixel-Based Change Detection Results Using Weighted Dempster–Shafer Theory. Remote Sensing, 12(6), 983. https://doi.org/10.3390/rs12060983

Jia, L., Li, M., Zhang, P., Wu, Y., & Zhu, H. (2016). SAR image change detection based on multiple kernel K-means clustering with local-neighborhood information. IEEE Geoscience and Remote Sensing Letters, 13(6), 856-860.

Lee, J.-S. (1981). Speckle analysis and smoothing of synthetic aperture radar images. Computer graphics and image processing, 17(1), 24-32.

Li, H.-C., Celik, T., Longbotham, N., & Emery, W. J. (2015). Gabor feature based unsupervised change detection of multitemporal SAR images based on two-level clustering. IEEE Geoscience and Remote Sensing Letters, 12(12), 2458-2462.

Li, M., Li, M., Zhang, P., Wu, Y., Song, W., & An, L. (2018). SAR image change detection using PCANet guided by saliency detection. IEEE Geoscience and Remote Sensing Letters, 16(3), 402-406.

Li, Q., Gong, H., Dai, H., Li, C., He, Z., Wang, W., … Mu, T. (2021). Unsupervised Hyperspectral Image Change Detection via Deep Learning Self-Generated Credible Labels. IEEE Journal of

Selected Topics in Applied Earth Observations and Remote Sensing, 14, 9012-9024. https://doi.org/10.1109/JSTARS.2021.3108777

Li, Y., Ren, J., Yan, Y., Liu, Q., Petrovski, A., & McCall, J. (2022). Unsupervised Change Detection in Hyperspectral Images using Principal Components Space Data Clustering. Journal of Physics : Conference Series, 2278(1), 012021. https://doi.org/10.1088/1742-6596/2278/1/012021

Liu, Q., Liu, L., & Wang, Y. (2017). Unsupervised Change Detection for Multispectral Remote Sensing Images Using Random Walks. Remote Sensing, 9(5), 438. https://doi.org/10.3390/rs9050438

Lou, X., Jia, Z., Yang, J., & Kasabov, N. (2019). Change Detection in SAR Images Based on the ROF Model Semi-Implicit Denoising Method. Sensors, 19(5), 1179. https://doi.org/10.3390/s19051179

Lv, Z., Liu, T., Shi, C., Benediktsson, J. A., & Du, H. (2019). Novel Land Cover Change Detection Method Based on k-Means Clustering and Adaptive Majority Voting Using Bitemporal Remote Sensing Images. IEEE Access, 7, 34425-34437. https://doi.org/10.1109/ACCESS.2019.2892648

Saha, S., Bovolo, F., & Bruzzone, L. (2019). Unsupervised Deep Change Vector Analysis for Multiple-Change Detection in VHR Images. IEEE Transactions on Geoscience and Remote Sensing, 57(6), 3677-3693. https://doi.org/10.1109/TGRS.2018.2886643

Saha, S., Bovolo, F., & Bruzzone, L. (2020). Building change detection in VHR SAR images via unsupervised deep transcoding. IEEE Transactions on Geoscience and Remote Sensing, 59(3), 1917-1929.

Scheffler, D., Hollstein, A., Diedrich, H., Segl, K., & Hostert, P. (2017). AROSICS : An Automated and Robust Open-Source Image Co-Registration Software for Multi-Sensor Satellite Data. Remote Sensing, 9(7), 676. https://doi.org/10.3390/rs9070676

Seydi, S. T., Hasanlou, M., & Chanussot, J. (2021). DSMNN-Net: A Deep Siamese Morphological Neural Network Model for Burned Area Mapping Using Multispectral Sentinel-2 and Hyperspectral PRISMA Images. Remote Sensing, 13(24), Article 24. https://doi.org/10.3390/rs13245138

Wang, B., Choi, S., Byun, Y., Lee, S., & Choi, J. (2015). Object-Based Change Detection of Very High Resolution Satellite Imagery Using the Cross-Sharpening of Multitemporal Data. IEEE Geoscience and Remote Sensing Letters, 12(5), 1151–1155. https://doi.org/10.1109/LGRS.2014.2386878

Wang, S., You, H., & Fu, K. (2011). BFSIFT : A novel method to find feature matches for SAR image registration. *IEEE Geoscience and Remote Sensing Letters*, *9*(4), 649-653.

Wang, Z., Jiang, F., Liu, T., Xie, F., & Li, P. (2021). Attention-Based Spatial and Spectral Network with PCA-Guided Self-Supervised Feature Extraction for Change Detection in Hyperspectral Images. *Remote Sensing*, *13*(23), 4927. https://doi.org/10.3390/rs13234927

Wu, Y., Bai, Z., Miao, Q., Ma, W., Yang, Y., & Gong, M. (2020). A Classified Adversarial Network for Multi-Spectral Remote Sensing Image Change Detection. *Remote Sensing*, *12*(13), 2098. https://doi.org/10.3390/rs12132098